Adaptable Integrated Sensing and Communication for UAV-Empowered 6G Networks

Yan Yang, Jianwei Zhao, Feifei Gao, Weimin Jia and Di Mu

Integrated sensing and communication (ISAC) is a promising technique for unmanned aerial vehicle (UAV)-empowered 6G networks. In this letter, we propose a novel adaptable ISAC mechanism. Firstly, we investigate both the communication and sensing channel model under Doppler and beam-squint effect. Then, we propose an adaptive sensing method by the joint designing the signal echo sensing and beam-squint sensing under practical environment. Specifically, when the echo power is larger than the minimum detectable power, the proposed method could realize the effective sensing by utilizing the system model without feedback. Otherwise, the proposed method could exploit the beam-squint for sensing with the feedback of the sub-carrier index. Finally, various simulation results are provided to demonstrate the effectiveness of the proposed scheme.

Introduction: Integrated sensing and communication (ISAC) has attracted great research interest and attention in both the academia and the industry due to its enormous potential in future sixth generation (6G) wireless systems [1]. The preliminary works on ISAC mainly focus on terrestrial networks, which may experience severe performance degradation due to the inadequate infrastructure coverage, signal blockage from surrounding obstacles and so on [2]. Unmanned aerial vehicles (UAVs) can overcome these limitations and are expected to play crucial roles in 6G networks by fully exploiting the high maneuverability, rapid deployment and the low-cost [3]. The UAV base station (BS) with ISAC technology can not only provide timely enhanced communication services for ground users, but also improve the sensing performance through mutual cooperation [3, 4].

It is a challenging issue to achieve the precise sensing in the high mobility scenarios. The work [5] proposed an extended Kalman filter (EKF) based tracking method by utilizing the radar echoes. A factor graph model and a message passing algorithm was considered in [6] to achieve the same objective. However, in practical environment, the echo intensity would be significantly attenuated due to factors such as the adverse weather, interference, distance, and target radar cross-section (RCS), which directly affects the reliability of sensing. Authors of [7] exploited the beam-squint effect to make beams at the different subcarriers towards different directions, which expanded the sensing coverage.

In this paper, we propose a new adaptable ISAC mechanism for the UAV-empowered 6G networks, in which the echo sensing and beam-squint sensing are jointly designed for sensing enhancement. We firstly model the UAV channel under the Doppler and beam-squint effect with wideband massive multiple-input multiple-output (MIMO) systems in ISAC scenarios. Then, we propose an adaptable ISAC mechanism according to the echo signal power by fully taking the advantages of echo sensing and beam-squint sensing, which only requires a little overhead to improve sensing performance. Finally, we provide various simulation results to verify the effectiveness of the proposed method.

System Model: We consider an UAV-empowered ISAC system as shown in Fig. 1, where K vehicles with single antenna are served by one hovering UAV BS. The UAV BS operates at millimeter wave (mmWave) band equipped with the uniform linear arrays (ULAs), where N_t transmit antennas and N_r receive antennas are seperatively configured to ensure the uninterrupted downlink transmission and receive the echoes [6]. Besides, the ULAs are parallel to the road surface spaced with inter-antenna spacing $\ell = \frac{\lambda_c}{2}$. In addition, a hybrid architecture with a total of K RF chains is deployed at the UAV BS, with each RF chain connected to multiple antennas through multiple Phase Shifters (PSs). We divide the ISAC service period T into N time slots with a time slot length $n = \frac{T}{N}$, indexed by $n \in \{1, 2, \cdots, N\}$.

Transmit Signal Model: The UAV BS simultaneously transmits K dimensional multi-beam ISAC signals to K vehicles at time slot n, denoted as $\mathbf{s}_n(t) = [s_{1,n}(t), s_{2,n}(t), \cdots, s_{K,n}(t)]^T$. We assume that the signals transmit through line-of-sight (LoS) channels [5, 6], and the transmission signals over N_t antennas can be represented as $\tilde{\mathbf{s}}_n(t) = \mathbf{F}_n \mathbf{s}_n(t) \in \mathbb{C}^{N_t \times 1}$, where $\mathbf{F}_n \in \mathbb{C}^{N_t \times K}$ is the beamforming matrix. Denote the angle of departure (AoD), distance, and speed of vehicle k at time slot n as $\theta_{k,n}$, $d_{k,n}$ and $v_{k,n}$. The beamforming matrix $\mathbf{F}_n$ can be designed with the predicted angle $\hat{\theta}_{k,n|n-1}$ towards the vehicle. Then, the kth column of $\mathbf{F}_n$ can be represented as $\mathbf{f}_{k,n} = \mathbf{u}(\theta_{k,n}) \approx \mathbf{u}(\hat{\theta}_{k,n|n-1}), \forall k, n$, where $\mathbf{u}(\theta_{k,n})$ is the transmit steering vector corresponding to $\theta_{k,n}$.

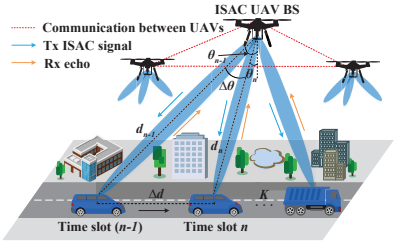

Fig. 1. The proposed UAV-empowered ISAC system.

Communication Model: Denote the transmission bandwidth and carrier frequency as F and f_c, respectively. Then, the propagation delay $\gamma_{k,m}$ from the mth ($m \in [1, N_t]$) antenna of UAV BS to vehicle k can be written as $\gamma_{k,m} = \gamma_{k,1} + (m-1) \cdot \frac{\ell \sin\theta_k}{c}$, where $\gamma_{k,1}$ is the propagation delay from vehicle k to the first antenna of the UAV BS. Denote $\xi_k \triangleq \frac{\ell \sin\theta_k}{\lambda_c}$, where λ_c and c represent the wavelength and the speed of light, respectively. The corresponding baseband signal of the mth antenna of the UAV BS with beam squint effect can be derived as [7]

$$y_{k,m}(t) = \beta_k e^{j2\pi\rho_k t} s_{k,m}\left(t - \gamma_{k,m}\right) e^{-j2\pi(m-1)\xi_k}, \quad (1)$$

where $\rho_k = \frac{v_k f_c}{c \sin\theta_k}$ represents the Doppler frequency of vehicle k; $\beta_k \triangleq \sqrt{N_t P_k}\alpha_k e^{-j2\pi f_c \gamma_{k,1}}$ is defined as equivalent baseband complex gain; P_k is the transmit power at the kth beam; $\alpha_k \triangleq \tilde{\alpha} d_k^{-1} e^{j\frac{2\pi f_c d_k}{c}}$ is the communication channel coefficient, and $\tilde{\alpha}$ is the channel power gain at the reference distance $d_0 = 1$m.

Then, the time-domain response of the downlink channel between the mth antenna of the UAV BS and vehicle k can be derived as $h_{k,m}(t) = \beta_k e^{j2\pi\rho_k t} e^{-j2\pi(m-1)\xi_k} \delta(t - \gamma_{k,1} - (m-1)\frac{\xi_k}{f_c})$, where $\delta(\cdot)$ denotes the Dirac delta function. The complex baseband frequency-domain response can be expressed as

$$h_{k,m}(f) = \beta_k e^{j2\pi\rho_k t} e^{-j2\pi(m-1)\xi_k(1+\frac{f}{f_c})} e^{-j2\pi f \gamma_{k,1}}, \quad (2)$$

where $f \in [0, F]$. The transmit steering vector corresponding to AoD θ_k is given by $\mathbf{u}(\theta_k, f) = [1, e^{-j2\pi\xi_k(1+\frac{f}{f_c})}, \cdots, e^{-j2\pi(N_t-1)\xi_k(1+\frac{f}{f_c})}]^T$.

The frequency-domain channel between the UAV BS and vehicle k is further expressed as $\mathbf{h}_k(f) = \beta_k \mathbf{u}^H(\theta_k, f) e^{j2\pi\rho_k t} e^{-j2\pi f \gamma_{k,1}}$. According to Eq. (2), the signal received by vehicle k at frequency f is $y_k(f) = \sum_{m=1}^{N_t} h_{k,m}(f) s_{k,m}(f) + \kappa_k = [h_{k,1}(f), \cdots, h_{k,N_t}(f)][s_{k,1}(f), \cdots, s_{k,N_t}(f)]^T + \kappa_k = \mathbf{h}_k(f)^T \mathbf{s}_k(f) + \kappa_k$, where $s_{k,m}(f)$ is the frequency-domain signal transmitted by the mth antenna of the UAV BS, and $\kappa \in \mathcal{CN}(0, \sigma_k^2)$ is an additive Gaussian noise. It can be observed that the transmit steering vector $\mathbf{u}(\theta_k, f)$ is frequency dependent, and $\mathbf{u}(\theta_k, f)$ will change directions with different frequency f, which is called *beam-squint effect* [7, 8].

Assuming the ISAC signal $s_{k,n}(t)$ has unit power, the receive signal-to-noise ratio (SNR) for vehicle k at time slot n is given by $SNR_{k,n} = \frac{N_t P_{k,n} |\alpha_{k,n} \mathbf{u}^H(\theta_{k,n}, f) \mathbf{u}(\hat{\theta}_{k,n|\mathbf{n}-1})|^2}{\sigma^2}$. Furthermore, we can obtain the achievable rate of vehicle k at time slot n as $R_{k,n} = \log(1 + SNR_{k,n})$.

Echo Signal Model: Compared with the communication signal, the Doppler frequency and time delay of the echo signal are doubled due to the round-trip of the signal. Correspondingly, the vehicle echo received at time slot n can be modeled as [5, 6]

$$\mathbf{r}_n(t) = \eta_{k,n} \sum_{k=1}^{K} e^{j2\pi\mu_{k,n} t} \mathbf{v}\left(\theta_{k,n}\right) \mathbf{u}^H\left(\theta_{k,n}\right) \mathbf{f}_{k,n} \mathbf{s}_n\left(t - \tau_{k,n}\right) + \mathbf{z}_{r,n}(t), \quad (3)$$

where $\eta_{k,n} = \sqrt{N_t N_r P_{k,n}}\varepsilon_{k,n}$, $P_{k,n}$ is the transmit power at the kth beam at time slot n, and $\varepsilon_{k,n}$ represents the reflection coefficient of vehicle k. Note that the time delay $\tau_{k,n}$ here is a round-way delay, while the Doppler frequency is $\mu_{k,n} = \frac{2v_{k,n} f_c}{c \sin\theta_{k,n}}$. Moreover, $\mathbf{v}(\theta_{k,n}) = [1, e^{-j2\pi\xi_k(1+\frac{f}{f_c})}, \cdots, e^{-j2\pi(N_r-1)\xi_k(1+\frac{f}{f_c})}]^T$ represents the receive steering vector and $\mathbf{z}_{r,n}(t) \in \mathcal{CN}(0, \sigma_{r,n}^2)$ is the complex additive white Gaussian noise.

Since the different steering vectors are approximately orthogonal to each other under massive MIMO configuaration, the interference between the beams of echoes reflected by K vehicles can be omitted. Then, the echo received for vehicle k can be represented as $\mathbf{r}_{k,n}(t) = \eta_{k,n} e^{j2\pi\mu_{k,n}t}\mathbf{v}\left(\theta_{k,n}\right)\mathbf{u}^H\left(\theta_{k,n}\right)\mathbf{f}_{k,n}\mathbf{s}_{k,n}\left(t-\tau_{k,n}\right)+\mathbf{z}_{r,k,n}(t)$.

Adaptable ISAC with Echo and Beam-squint: The adaptable ISAC mechanism adopts a time division duplex model. We define $\psi_n \in \{0,1\}$ as the sensing indicator at time slot n, and the minimum detectable signal power of the UAV BS is denoted as $S_{\min}$. The sensing modes can be configured by setting the value of ψ_n. When the received echo power $P_{r,n}$ is larger than $S_{\min}$ at time slot n, we consider $\psi_n = 1$, which means that the UAV detects the vehicle echo and can extract its information from the echo. In the case of the harsh environments or being far away, it is difficult to use echoes to sense the target. As a result, there is $\psi_n = 0$, and beam-squint sensing will be utilized to fulfill continuous tracking. We will focus on estimating the angle of departure.

EKF based Sensing with Echo: We assume that the motion parameters remain constant within one time slot. For simplicity, the subscript k has been omitted for ease of annotation. According to the geometric relationship shown in Fig. 1, it holds that

$$\begin{cases} d_n^2 = d_{n-1}^2 + \Delta d^2 + 2d_{n-1}\Delta d\sin\theta_{n-1}, \\ d_n \sin\Delta\theta = \Delta d\cos\theta_{n-1}, \end{cases} \tag{4}$$

where $\Delta d = v_{n-1}\Delta T$, $\Delta\theta = \theta_n - \theta_{n-1}$. Then, we can approximate Eq. (4) as $d_n^2 - d_{n-1}^2 = (d_n + d_{n-1})(d_n - d_{n-1}) = \Delta d^2 + 2d_{n-1}\Delta d\sin\theta_{n-1}$.

The position of the vehicle will not change significantly within one time slot. Hence we have $d_n - d_{n-1} = \frac{\Delta d^2 + 2d_{n-1}\Delta d\sin\theta_{n-1}}{d_n + d_{n-1}} \approx \frac{\Delta d^2 + 2d_{n-1}\Delta d\sin\theta_{n-1}}{2d_{n-1}} = \Delta d(\frac{\Delta d}{2d_{n-1}} + \sin\theta_{n-1})$. Moreover, Δd can be ignored compared with d_{n-1}. Therefore, $\frac{\Delta d}{2d_{n-1}}$ can be approximately omitted, and there is $d_n \approx d_{n-1} + \Delta d\sin\theta_{n-1} = d_{n-1} + v_{n-1}\Delta T\sin\theta_{n-1}$. It holds that $\Delta\theta \approx \sin\Delta\theta = \frac{\Delta d\cos\theta_{n-1}}{d_n} = \frac{\Delta d\cos\theta_{n-1}}{d_{n-1}+\Delta d\sin\theta_{n-1}}$. Due to $\Delta d \ll d_{n-1}$ and $\Delta\theta = \theta_n - \theta_{n-1}$, we have $\theta_n \approx \theta_{n-1} + d_{n-1}^{-1}\Delta d\cos\theta_{n-1} = \theta_{n-1} + d_{n-1}^{-1}v_{n-1}\Delta T\cos\theta_{n-1}$.

We assume that the speed of the vehicle remains constant within one time slot, i.e., $v_n \approx v_{n-1}$. The state evolution model can be summarized as

$$\begin{cases} \theta_n = \theta_{n-1} + d_{n-1}^{-1}v_{n-1}\Delta T\cos\theta_{n-1} + \omega_\theta, \\ d_n = d_{n-1} + v_{n-1}\Delta T\sin\theta_{n-1} + \omega_d, \\ v_n = v_{n-1} + \omega_v, \end{cases} \tag{5}$$

where ω_θ, ω_d and ω_v denote the corresponding system noises, which are assumed as $\omega_\theta \in \mathcal{CN}(0,\sigma_\theta^2)$, $\omega_d \in \mathcal{CN}(0,\sigma_d^2)$ and $\omega_v \in \mathcal{CN}(0,\sigma_v^2)$.

According to the echo signal processing theroy, the measurement models for AoD θ_n and distance d_n can be written as [9]

$$\begin{cases} \tau_n = \dfrac{2d_n}{c} + z_\tau, \forall n, \\ \mu_n = \dfrac{2v_n f_c}{c\sin\theta_n} + z_\mu, \forall n, \end{cases} \tag{6}$$

where the noise terms z_τ and z_μ both satisfy the distribution $\mathcal{CN}(0,\sigma_\tau^2)$ and $\mathcal{CN}(0,\sigma_\mu^2)$.

Let us define the system states and measurement signal models as $\mathbf{x} = \left[\theta, d, v\right]^T$ and $\mathbf{y} = [\tau,\mu]^T$. Then, the models developed in (5) and (6) can be formulated in the compact forms as

$$\begin{cases} \text{State Evolution Model}: \mathbf{x}_n = \mathbf{g}(\mathbf{x}_{n-1}) + \boldsymbol{\omega}_n, \\ \text{Measurement Model}: \mathbf{y}_n = \mathbf{h}(\mathbf{x}_n) + \mathbf{z}_n, \end{cases} \tag{7}$$

where $\mathbf{g}(\cdot)$ is defined in (5), and $\mathbf{h}(\cdot)$ is defined in (6). Besides, the system noise vector $\boldsymbol{\omega} = \left[\omega_\theta, \omega_d, \omega_v\right]^T$ and the measurement noise vector $\mathbf{z} = [z_\tau, z_\mu]^T$ are independent to $\mathbf{g}(\mathbf{x}_{n-1})$ and $\mathbf{h}(\mathbf{x}_n)$, respectively. Both $\boldsymbol{\omega}$ and $\mathbf{z}$ obey the Gaussian distribution with zero-mean, and their covariance matrices can be written separately as $\mathbf{Q}_\omega = \mathrm{diag}\left(\sigma_\theta^2, \sigma_d^2, \sigma_v^2\right)$ and $\mathbf{Q}_z = \mathrm{diag}\left(\sigma_\tau^2, \sigma_\mu^2\right)$.

Due to the nonlinearity of (6), we use the EKF algorithm to linearize the nonlinear model. Then, the system states can be recursively derived from the consecutive cycles of predicting and updating, and the specific steps are are outlined below.

When the vehicle enters the coverage range of the UAV BS, the UAV BS transmits signals and detects echo intensity P_r^0. Then, the initial state information $\hat{\mathbf{x}}^0 = [\hat{\theta}^0, \hat{d}^0, \hat{v}^0]^T$ can be obtained by echo processing. Meanwhile, the prior mean square error (MSE) matrix can be set to $\mathbf{P}^0 = \mathbf{0}_{3\times 3}$.

With simple algebraic manipulation, the Jacobian matrix for $\mathbf{g}(\mathbf{x})$ and $\mathbf{h}(\mathbf{x})$ can be given by

$$\frac{\partial \mathbf{g}}{\partial \mathbf{x}} = \begin{bmatrix} 1 - \frac{v\Delta T\sin\theta}{d} & -\frac{v\Delta T\cos\theta}{d^2} & \frac{\Delta T\cos\theta}{d} \\ v\Delta T\cos\theta & 1 & \Delta T\sin\theta \\ 0 & 0 & 1 \end{bmatrix}, \tag{8a}$$

$$\frac{\partial \mathbf{h}}{\partial \mathbf{x}} = \begin{bmatrix} 0 & \frac{2}{c} & 0 \\ -\frac{2vf_c}{c\sin\theta\tan\theta} & 0 & \frac{2f_c}{c\sin\theta} \end{bmatrix}. \tag{8b}$$

Therefore, the linearization results can be obtained as $\mathbf{G}_{n-1} = \frac{\partial \mathbf{g}}{\partial \mathbf{x}}\Big|_{\mathbf{x}=\hat{\mathbf{x}}_{n-1}}, \mathbf{H}_n = \frac{\partial \mathbf{h}}{\partial \mathbf{x}}\Big|_{\mathbf{x}=\hat{\mathbf{x}}_{n|n-1}}$. The predicted system state can be obtained as $\hat{\mathbf{x}}_{n|n-1} = \mathbf{g}\big(\hat{\mathbf{x}}_{n-1}\big)$, while the predicted MSE matrix can be derived as $\mathbf{P}_{n|n-1} = \mathbf{G}_{n-1}\mathbf{P}_{n-1}\mathbf{G}_{n-1}^H + \mathbf{Q}_\omega$.

The Kalman gain matrix can be computed as $\mathbf{K}_n = \mathbf{P}_{n|n-1}\mathbf{H}_n^H\left(\mathbf{Q}_z + \mathbf{H}_n\mathbf{P}_{n|n-1}\mathbf{H}_n^H\right)^{-1}$. Then, the MSE matrix $\mathbf{P}_n$ can be generated as $\mathbf{P}_n = (\mathbf{I} - \mathbf{K}_n\mathbf{H}_n)\mathbf{P}_{n|n-1}$. Meanwhile, the system state $\hat{\mathbf{x}}_n$ can be updated as $\hat{\mathbf{x}}_n = \hat{\mathbf{x}}_{n|n-1} + \mathbf{K}_n(\mathbf{y}_n - \mathbf{h}(\hat{\mathbf{x}}_{n|n-1}))$, where $\mathbf{y}_n - \mathbf{h}(\hat{\mathbf{x}}_{n|n-1})$ represents the innovation of the measurement state. Moreover, the transmit beamforming vector based on predicted angle $\hat{\theta}_{n|n-1}$ can designed to point the beam towards the target vehicle at time slot n.

Sensing with Beam-Squint Effect: It is difficult to achieve a better sensing performance when the echo signal strength is insufficient for accurate detection. Let us consider beam-squint sensing when echoes cannot be used for sensing. Assuming ϕ_k is the angle intended to achieve beamforming, the phase of N_t PSs should be selected as $\mathbf{u}(\phi_k)^* = [1, e^{j2\pi\phi_k}, \cdots, e^{j2\pi(N_t-1)\phi_k}]^T$. Then, the array gain at frequency f can be given by

$$\left|\mathbf{u}^T(\theta_k, f)\mathbf{u}(\phi_k)^*\right| = \left|\sum_{m=1}^{N_t} e^{-j2\pi(m-1)\xi_k(1+\frac{f}{f_c})} \cdot e^{j2\pi(m-1)\phi_k}\right|. \tag{9}$$

Only when $\xi_k = \phi_k(1+\frac{f}{f_c})^{-1}$, the array gain in Eq. (9) can reach its maximum value. Furthermore, the beam-squint range within transmission bandwidth F can be calculated as $\Delta\xi_k = \phi_k\left(1 - (1+\frac{F}{f_c})^{-1}\right) = \phi_k\frac{F}{f_c+F}$.

In order to make the beam-squint range adaptive, we deploy the values of true-time-delay (TTD) lines between the PSs and the antennas to control the propagation delay [7]. Then, we obtain the frequency-domain response under the combination of the mth TTD line and the mth PS connected to the kth RF chain as $b_{k,m} = e^{j2\pi(m-1)\phi_k} \cdot e^{-j2\pi f t_{k,m}}$, where $t_{k,m}$ is the time delay introduced by TTD line m. The corresponding response vector can be derived as $\mathbf{b}_k = [b_{k,1}, b_{k,2}, \cdots, b_{k,N_t}]^T$.

We plan to make the subcarrier beamforming direction varies from the initial angle θ_0 to the termination angle θ_F as the frequency f increases from 0 to F. When the echo cannot be utilized to extract target information and beam-squint is enabled to realize sensing, we set the initial angle θ_0 according to the predicted target angle $\theta_{k,n-1}$ by the echo sensing at the previous moment. Under the wideband assumption, the array gain of $\mathbf{b}_k$ and $\mathbf{u}(\theta_k, f)$ is

$$\left|\mathbf{u}^T(\theta_k, f)\mathbf{b}_k\right| = \left|\sum_{m=1}^{N_t} e^{-j2\pi(m-1)(1+\frac{f}{f_c})\xi_k} e^{j2\pi(m-1)\phi_k} e^{-j2\pi f t_{k,m}}\right|. \tag{10}$$

Assuming the initial angle is θ_0 at subcarrier frequency $f = 0$, we obtain $\mathbf{u}(\theta_0, 0) = \frac{\sin\theta_0}{2}$. Substituting $\mathbf{u}(\theta_0, 0)$ back to Eq. (10), the array gain at $f = 0$ is given by $\left|\mathbf{u}^T(\theta_0, 0)\mathbf{b}_k\right| = \left|\sum_{m=1}^{N_t} e^{-j\pi(m-1)\sin\theta_0} e^{j2\pi(m-1)\phi_k}\right|$. To maximize the gain at $f = 0$, ϕ_k should take the value $\phi_k = \frac{\sin\theta_0}{2}$. Furthermore, the the initial angle θ_0 can be set to $\theta_0 = \arcsin(2\theta_{k,n-1})$.

Assuming the termination angle is θ_F at $f = F$, the transmit steering vector is given by $\mathbf{u}(\theta_F, F) = \frac{\sin\theta_F}{2}(1+\frac{F}{f_c})$. Substituting $\phi_k = \frac{\sin\theta_0}{2}$ and $\mathbf{u}(\theta_F, F)$ back to Eq. (10), the array gain at $f = F$ can be taken as $\left|\mathbf{u}^T(\theta_F, F)\mathbf{b}_k\right| = \left|\sum_{m=1}^{N_t} e^{-j\pi(m-1)\left((1+\frac{F}{f_c})\sin\theta_F - \sin\theta_0\right)} e^{-j2\pi F t_{k,m}}\right|$.

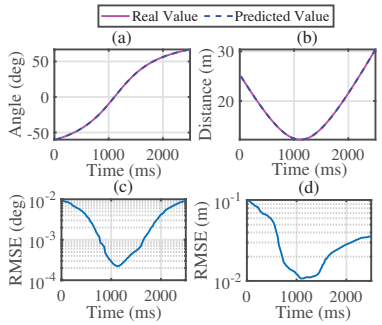

Fig. 2. Performances of the adaptable ISAC.

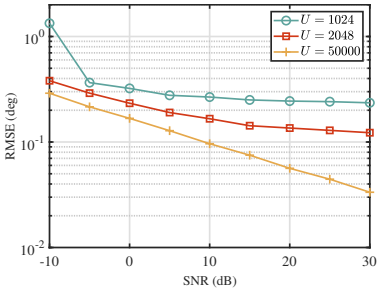

Fig. 3. RMSE of the sensing method with beam-squint versus SNR.

Therefore, the time delay $t_{k,m}$ corresponding to the mth TTD line needs to satisfy $t_{k,m}=\frac{m-1}{2F}(\sin\theta_0-\sin\theta_F(1+\frac{F}{f_c}))$ for the purpose of making the array gain reach its maximum value. The beamforming direction of the subcarrier beam at frequency f can be obtained as

$$\theta_k = \arcsin\left(\frac{\sin\theta_0 + \frac{f}{F}(\sin\theta_F(1+\frac{F}{f_c}) - \sin\theta_0)}{1+\frac{f}{f_c}}\right). \quad (11)$$

It can be observed that as the subcarrier frequency f increases, the beamforming angle θ_k of RF chain k will monotonically vary from θ_0 to θ_F. By pointing each subcarrier beam towards different direction simultaneously, the UAV BS can sense vehicles within the range $[\theta_0, \theta_F]$. Then, the vehicle located within the range will feedback the subcarrier frequency f with the maximum array gain to the UAV BS, and its direction can be calculated via Eq. (11). By fully utilizing the advantages of joint echo sensing and beam-squint sensing, the proposed scheme can significantly improve environmental adaptability and achieve continuous tracking.

Simulation Results: In this section, simulations are provided to verify the performance of the proposed scheme. We consider $F = 6$ GHz and $f_c = 30$ GHz. The transmission epoch length is set to $\Delta T = 20$ ms. For the noise of the state evolution model, we have $\sigma_\theta = 0.02°$, $\sigma_d = 0.2$ m and $\sigma_v = 0.5$ m/s. For the observed delays and Dopplers at UAV BS, we use the standard deviations of $\sigma_\tau = 0.3\ \mu s$ and $\sigma_\mu = 1$ kHz for the vehicle at different time slots.

In Fig. 2, we consider the tracking performance analysis of angle and distance with the adaptable ISAC scheme. We set the initial state of the vehicle to $\theta_0 = -60°$, $d_0 = 25$ m, $v_0 = 20$ m/s. The actual and predicted values of angle and distance are shown in Fig. 2(a) and Fig. 2(b). To evaluate the prediction accuracy, the corresponding root mean square error (RMSE) curves are also shown in Fig. 2(c) and Fig. 2(d). It can be observed that the RMSE of angle and distance all decrease when the vehicle approaches the UAV BS, and increase when it moves away. When the vehicle travels directly below the UAV BS, i.e., at the point where is around 1100 ms when $\theta = 0°$, the RMSE of the angle and distance with the adaptable ISAC reaches the minimum value.

In Fig. 3, the RMSE based on beam-squint sensing method is plotted on SNR, where $N_t = 128$. We consider that the angle range and sensing range of AoD are both $-80°$ to $80°$. When the number of subcarriers U is small, the sensing accuracy performance is poor at low SNR. It can be found that as the number of subcarriers U increases, the sensing accuracy significantly improves. By increasing the number of subcarriers U, the grid division can become more dense, which will lead to higher sensing accuracy.

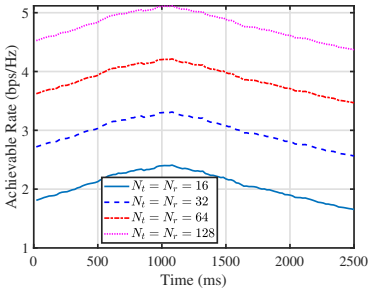

Fig. 4. Achievable rate versus time, SNR = 10 dB.

Fig. 4 shows the variation of achievable communication rate over time considering Doppler effect and beam-squint effect, where SNR = 10 dB. We can observe that due to the change in distance between the vehicle and the UAV BS, all achievable communication rate curves increase initially and then decrease. When the vehicle is closest to the UAV BS projection, the maximum communication rate can be achieved, i.e., at the point where $\theta = 0°$. In addition, it can be found that by increasing the number of transmit and receive antennas, the achievable communication rate is improved thanks to the enhancement in array gain.

Conclusion: In this letter, we designed a novel adaptable ISAC mechanism, which jointly exploits echo sensing and beam-squint sensing for UAV-empowered mmWave massive MIMO systems. Specially, UAVs could flexibly switch sensing modes under practical requirements, which effectively addresses the limitations of only echo sensing and provides a new paradigm for sensing in the harsh environments. Besides, only a little overhead is required during the feedback stage of beam-squint sensing, which reduces the system overhead. Finally, we provided simulation results to show the effectiveness of the proposed scheme.

Acknowledgment: This research was sponsored by the National Natural Science Foundation of China (grant no. 62001500).

Y. Yang, J. Zhao and W. Jia are with High-Tech Institute of Xi'an, Xi'an, Shaanxi 710025, China. F. Gao is with Tsinghua National Laboratory for Information Science and Technology (TNList) and the Beijing Key Laboratory of Mobile Computing and Pervasive Device, Institute of Computing Technology, Chinese Academy of Sciences, Beijing 100084, China. D. Mu is with Beijing Institute of Radio Measurement, Beijing 100854, China.

E-mail: zhaojw15@mails.tsinghua.edu.cn(zhaojianweiep@163.com)

References

1 A. Liu *et al.*, "A survey on fundamental limits of integrated sensing and communication," *IEEE Commun. Surv. Tutor.*, vol. 24, no. 2, pp. 994-1034, Feb. 2022.

2 C. Deng, X. Fang, and X. Wang, "Beamforming design and trajectory optimization for UAV-empowered adaptable integrated sensing and communication," *IEEE Trans. Wirel. Commun.*, early access, 2023.

3 J. Zhao, F. Gao, W. Jia, W. Yuan, and W. Jin, "Integrated sensing and communications for UAV communications with jittering effect," *IEEE Wirel. Commun. Lett.*, vol. 12, no. 4, pp. 758-762, Apr. 2023.

4 Z. Fei, X. Wang, N. Wu, J. Huang and J. A. Zhang, "Air-ground integrated sensing and communications: opportunities and challenges," *IEEE Commun. Mag.*, vol. 61, no. 5, pp. 55-61, May 2023.

5 F. Liu, W. Yuan, C. Masouros, and J. Yuan, "Radar-assisted predictive beamforming for vehicular links: communication served by sensing," *IEEE Trans. Wirel. Commun.*, vol. 19, no. 11, pp. 7704-7719, Nov. 2020.

6 W. Yuan, F. Liu, C. Masouros, J. Yuan, D. W. K. Ng, and N. Gonzalez-Prelcic, "Bayesian predictive beamforming for vehicular networks: a low-overhead joint radar-communication approach," *IEEE Trans. Wirel. Commun.*, vol. 20, no. 3, pp. 1442–1456, Mar. 2021.

7 F. Gao, L. Xu, and S. Ma, "Integrated sensing and communications with joint beam-squint and beam-split for mmWave/THz massive MIMO," *IEEE Trans. Commun.*, vol. 71, no. 5, pp. 2963–2976, May 2023.

8 Y. Chen, Y. Xiong, D. Chen, T. Jiang, S. X. Ng and L. Hanzo, "Hybrid Precoding for WideBand Millimeter Wave MIMO Systems in the Face of Beam Squint," *IEEE Trans. Wirel. Commun.*, vol. 20, no. 3, pp. 1847-1860, Mar. 2021.

9 J. Wu, W. Yuan, F. Liu, Y. Cui, X. Meng and H. Huang, "UAV-Based Target Tracking: Integrating Sensing into Communication Signals," in *Proc. IEEE/CIC Int. Conf. Commun. China (ICCC Workshops)*, 2022, pp. 309-313.